The ORNL-SNAP Shielding Program

F. R. Mynatt, C. E. Clifford, F. J. Muckenthaler, and M. L. Gritzner
Oak Ridge National Laboratory

The effort in the ORNL-SNAP shielding program is directed toward the development and verification of computer codes using numerical solutions to the transport equation for the design of optimized radiation shields for SNAP power systems. A brief discussion is given for the major areas of the SNAP shielding program, which are cross-section development, transport code development, and integral experiments. Detailed results are presented for the integral experiments utilizing the TSF-SNAP reactor. Calculated results are compared with experiment for neutron and gamma-ray spectra from the bare reactor and as transmitted through slab shields.

The purpose of the ORNL-SNAP shielding program is the development of the technology for the nuclear design of radiation shields for reactor power supply systems on spacecraft. The emphasis in the program is on the development and verification of computer programs for the design of optimum shields and to predict throughout the spacecraft system the absolute spectra of radiation resulting from reactor operation.

Figure 1 shows a schematic diagram of the SNAP shielding program. The three major areas which are shown are cross-section development, transport code development and integral experiments. Five years ago the calculation of deep-penetration neutron transport in lithium hydride in a one-dimensional geometry was a challenging problem. The capabilities since that time have increased rapidly.

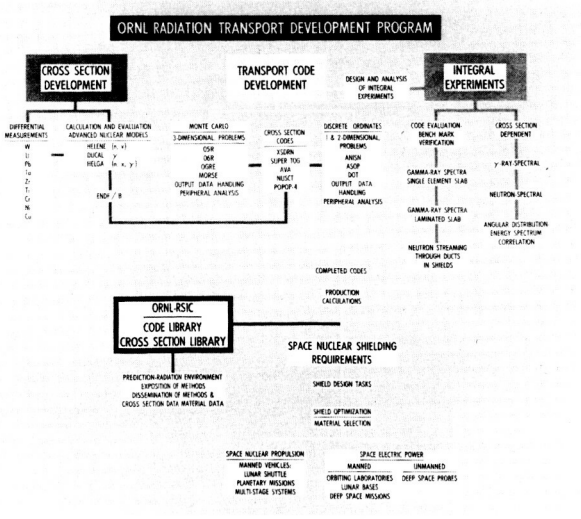

FIGURE 1.-A Schematic Description of the ORNL-SNAP Shielding Program.

The significant steps in this development include (1) the ability to calculate neutron and secondary gamma-ray transport in a coupled mode, (2) the development of the DOT (refs. 1 and 2) discrete ordinates code for deep-penetration two-dimensional transport calculations, (3) the development of a shield optimization program, ASOP (ref. 3), utilizing one-dimensional transport calculations, and (4) the development of the multigroup Monte Carlo MORSE (ref. 4) and the coupling of MORSE and two-dimensional DOT calculations for the analysis of difficult two- and three-dimensional problems.

The current development work includes MORSE-DOT coupling and the optimum shaping of shields which is a rudimentary form of multidimensional optimization. The verification of the shield design and analysis methods is effected through comparison with integral experiments. Two types of integral experiments have been performed at the ORNL Tower Shielding Facility. In the first type of experiment the measurements are of absolute gamma-ray pulse-height spectra produced from thin slabs which are exposed to a filtered neutron beam. In comparison with this experiment, the calculation of transport effects is minimized and the emphasis is placed on the calculation of the production of secondary gamma rays (refs. 5 and 6).

The second type of exeriment is more prototypical in that absolute neutron and gamma-ray spectra transmitted from slab shields placed adjacent to the TSF-SNAP reactor are compared. These comparisons test the transport calculation of neutrons and gamma rays, as well as the production of secondary gamma rays. In the comparison with integral experiments, it was soon verified that the available cross-section data for production of secondary gamma rays were grossly inadequate for most materials. This situation has now been greatly improved in that data for production of secondary gamma rays

from neutron capture as a function of neutron energy have been produced by use of nuclear model theory codes (refs. 7 and 8) and by measurements for tungsten (ref. 9) and uranium (ref. 10). Current work is directed toward the verification and improvement of data for secondary gamma-ray production due to neutron inelastic scattering.

As the techniques developed in the basic technology program have become established, they have been incorporated in an optimum-shield-design procedure which is exercised and demonstrated through detailed shield design studies. Several studies have been performed in which the reactor type and power and the radiation dose constraints are specified and an optimized shield is designed (ref. 11). Through these efforts, the techniques for shield design are being rapidly improved.

Also of interest are parametric optimization studies in which the effect of reactor size, type and power and the radiation dose constraints on the optimum shield configuration and weight have been studied. These studies, of course, incorporate considerable simplification of the geometry as compared to the more detailed design studies for a specific configuration.

Other papers by the ORNL group at this meeting will cover, in more detail, the integral experiments for secondary gamma-ray data testing (ref. 12), the use of coupled MORSE Monte Carlo and DOT calculations for three-dimensional problems (refs. 13 and 14), and the design of optimized shaped asymmetric 4π shields (ref. 15). In this paper, the status of the calculational comparisons with the TSF-SNAP integral experiments will be summarized.

The source for these experiments is the TSF-SNAP reactor shown before assembly in figure 2. The reactor is a modified SNAP-2 which was designed and constructed by Atomics International. The pressure vessel shown on the left is 9 in. in diameter, 16 in. long, and contains the uranium-zirconium-hydride fuel in 36 rods with a central stainless steel rod containing a small quantity of boron carbide. The reactor is reflected radially by beryllium and has four reflector control vanes. The coolant is NaK and the heat is removed by natural circulation to a NaK-to-air heat exchanger above the reactor. In the dry critical runs during the

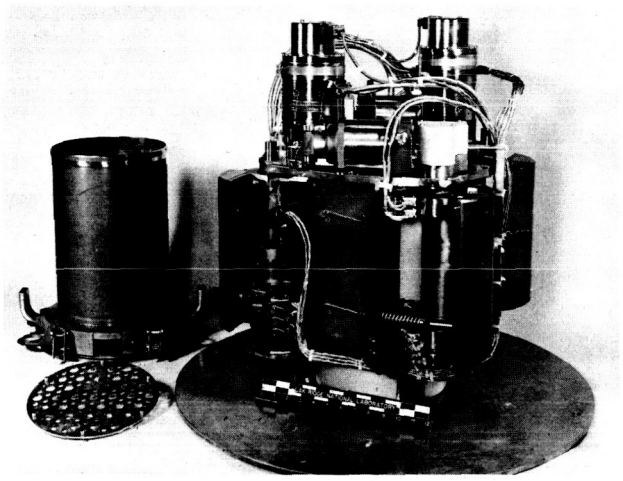

FIGURE 2.-The TSF-SNAP Reactor Prior to Assembly.

start of the reactor, the internal power distribution was measured by gamma-ray scans of the fuel elements, by copper, uranium, and gold foil activation and by activation of copper strips. Comparisons of the power distribution deduced from these measurements with 05R-Monte Carlo calculations and DOT discrete ordinates calculations show very good agreement for the radial and axial power distributions (ref. 16).

After the assembly of the reactor was completed and in its final operating stage, the first measurements which were made were of the neutron angular current leaking from the bottom of the assembly. Figure 3 shows the SNAP reactor without the heat shield suspended from its boom. The large collimator tank contains a special 2-in. by 2-in. square collimator which was designed to view only 10% of the area of the core. By moving the collimator along the track and varying the angle position, several measurements were made of the angle-dependent neutron leakage. Data from this experiment showed that except for those measurements where the collimator was vertical and viewing the outer extremity of the core and reflector, the spectral shape and intensity which were measured were very similar for each run. Comparisons of the measured absolute spectra with very detailed 05R calculations showed substantially good agreement (ref. 17).

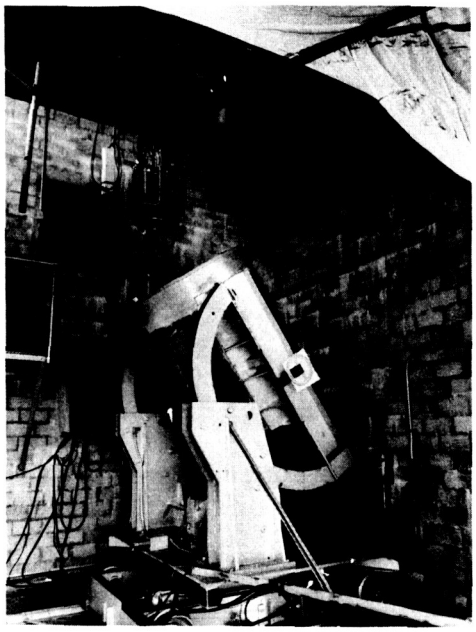

FIGURE 3.-TSF-SNAP Reactor With NE-213 Detector Collimator Used For Measurement of the Angle-Dependent Neutron Leakage.

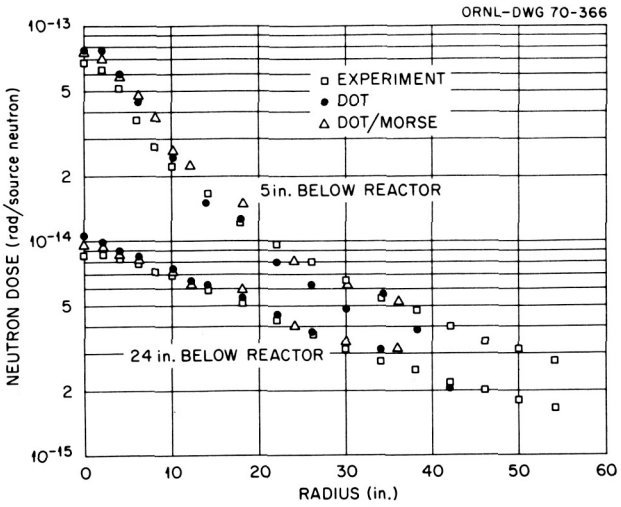

FIGURE 4.-Comparison of Calculated and Measured Radial Neutron Dose Profiles Below the SNAP Reactor.

Figure 4 shows comparison of measurements and calculations for lateral neutron dose traverses below the SNAP reactor. The measurements were made with a small Hornyak button, and the calculations were made with the two-dimensional DOT code for the reactor coupled, in one case with the SPACETRAN ray-tracing code to obtain the dose at the specified points, and in the other case the coupling at a plane just below the reactor was made to the MORSE Monte Carlo code which then determined the dose at the specified points. The agreement between the calculations and experiment is surprisingly good. In the DOT-SPACETRAN coupling, however, some ray effects can be observed for large radii on the plane close to the bottom of the reactor.

Additional neutron and gamma-ray spectral measurements for the bare reactor are included in the slab shield transmission series. The neutron and gamma-ray slab transmission measurements have been performed with large slab shields supported such that they are located directly under the SNAP reactor. Measurements have been made with the NE-213 fast-neutron scintillator and the sodium-iodide gamma-ray detector.

Figure 5 shows a list of the experiments for which calculations have been performed. There are many other experimental runs which have been made but not yet calculated. From figure 5 you can see that neutron measurements and calculations have been performed for the bare reactor, and lithium-hydride, depleted uranium, lead, tungsten powder, heavimet alloy, and laminated lithium-hydride lead-uranium slabs. More difficult gamma-ray measurements and calculations have been performed for the bare reactor, and lead, depleted uranium, heavimet alloy, tungsten powder, and laminated lithium-hydride and uranium slabs.

Figure 6 shows a scale drawing of the geometric configuration for the fast-neutron spectral measurements. The NE-213 detector is located deep in a room beneath the concrete pad. The area of the slab which it views is defined by the inner wall of the water tank. In the calculations, the leakage angular flux from a DOT calculation of the reactor is used as a boundary source for the calculation of the slab shield. The leakage angular flux from the bottom of the slab shield is then integrated with SPACETRAN code to obtain the absolute neutron flux

at the NE-213 detector. In the experiment, the pulse-height distribution from the NE-213 is unfolded with the FERDOR code and compared with the calculation at the detector point. The comparisons are always on an absolute basis with the reactor power monitored by foils during each run.

EXPERIMENTS WHICH HAVE BEEN CALCULATED

NEUTRON	GAMMA
BARE REACTOR	BARE REACTOR
6" LiH	2" Pb
12" LiH	3" Pb
1.5" U-238[a]	6" Pb
4.5" U-238	3.5" U-238
1.5" Pb	4.5" U-238
3" Pb	2" HEAVIMET
6" W[b]	6" W
12" W	6" LiH-1.5" U-238
2" HEAVIMET[c]	
1.5" U-238-6" LiH	
6" LiH-1.5" U-238	
6" LiH-1.5" Pb-1.5" U-238	
6" LiH-4.5" U-238	
6" LiH-1.5" Pb	
3" Pb-6" LiH	

[a] U-238 is depleted uranium.
[b] W is tungsten powder ($\rho \sim 6$ gm./cm.^{3}).
[c] HEAVIMET is tungsten-copper-nickel alloy.

FIGURE 5.-A List of TSF-SNAP Slab Transmission Experiments Which Have Been Calculated.

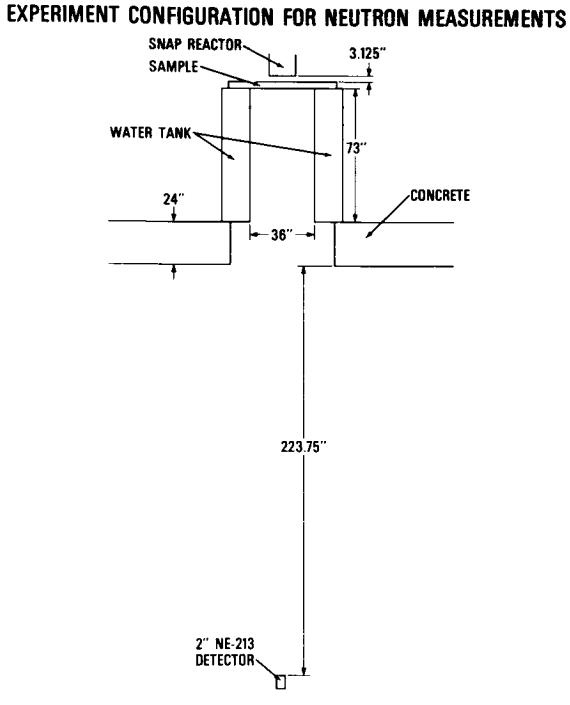

FIGURE 6.-Experimental Configuration for Fast-Neutron Measurements.

Figure 7 shows a comparison of experiment with DOT-SPACETRAN calculation and Monte Carlo 05R calculation for the fast-neutron spectra for the bare core. The agreement is very good except that the calculations are somewhat high below 1-1/2 MeV.

Figure 8 shows a comparison of DOT calculation with a recent measurement of the neutron leakage from the bare core using the Benjamin spectrometer which uses spherical hydrogen-filled detectors. The measurements were made at approximately 36 in. below the reactor core. The calculation uses DOT coupled with SPACETRAN in the usual manner, and the agreement in intensity is quite good except that the calculation is somewhat high between 600 keV and 1-1/2 MeV. Also shown is the result of scaling the NE-213 measurements to the hydrogen counter location. The agreement between the NE-213 spectrometer and the Benjamin spectrometer in the overlap energy range is excellent.

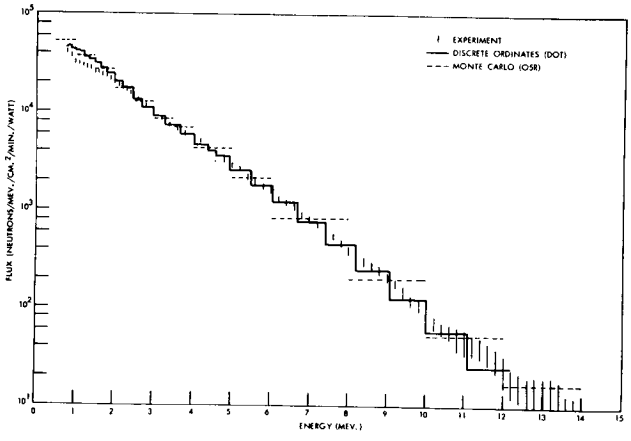

FIGURE 7.-Comparison of Calculated and Measured Fast-Neutron Spectra From the Bare TSF-SNAP Reactor.

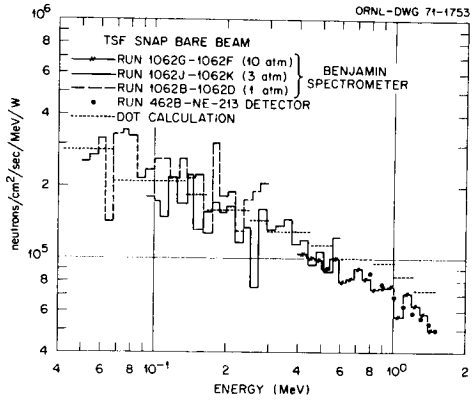

FIGURE 8.-Comparison of Calculated and Measured Intermediate Neutron Spectra From the Bare TSF-SNAP Reactor.

Figure 9 shows a comparison of measurement with DOT and 05R calculations for a 12-in.-thick slab of lithium hydride. The overall agreement is very good; however, the calculations are somewhat high below 2 MeV and somewhat low at the higher energies. The multigroup lithium cross sections used in the DOT calculation were processed prior to the availability of lithium in the ENDF/B library but used the same data as used for the ENDF evaluation. It is important that all of the neutron-producing reactions in lithium be treated in order to obtain reasonably good agreement. In this multigroup set, the secondary neutron distributions from the nonelastic reactions are assumed to be isotropic in the laboratory system. However, in the Monte Carlo calculation the angular distributions of the secondary neutrons are treated explicitly. Previous comparisons in one-dimensional sphere geometry between 05R and multigroup ANISN calculations have shown excellent agreement in lithium hydride to a depth of 90 cm (ref. 18).

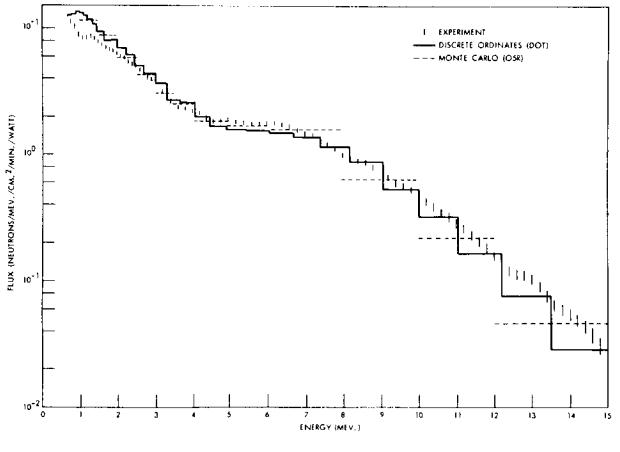

FIGURE 9.-Comparison of Measured and Calculated Fast-Neutron Spectra From a 12-in. Lithium Hydride Slab Under the SNAP Reactor.

Figure 10 shows a comparison of experiment and DOT calculation for the fast-neutron spectra transmitted through a 2-in. slab of heavimet alloy. The agreement for this case is the best for any of the metal slabs which have been calculated. For lead, the calculated spectra are consistently 15% low, and for uranium at large slab thicknesses the calculations are a factor of 2 to 2-1/2 low. This result for uranium is anomolous since comparisons of DOT calculations with experiment using the same slabs in a beam source geometry have previously shown good agreement when the fission multiplication in the slab is treated (ref. 1, page 144). Experiments are currently in progress to attempt to determine the reason for this disagreement in this case.

Figure 11 shows a scale drawing of the geometry for the gamma-ray measurements and calculations. The 5-in. sodium iodide detector is also located deep in the room beneath the concrete pad. In the gamma-ray measurements a 10-in. thickness of borated polyethylene is in the beam at all times to reduce the neutron background in the detector.

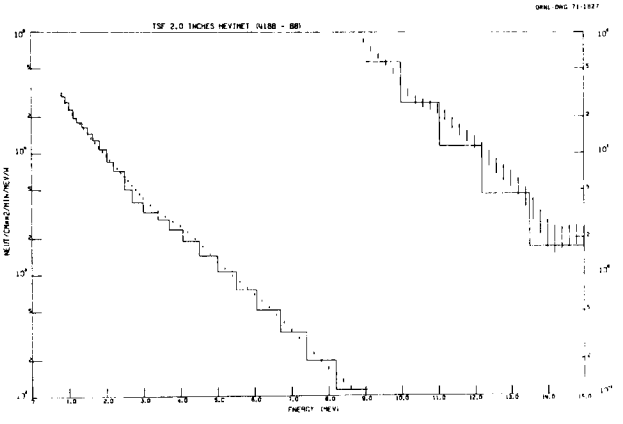

FIGURE 10.-Comparison of Calculated and Measured Fast-Neutron Spectra From a 2-in. Slab of Heavimet Under the SNAP Reactor.

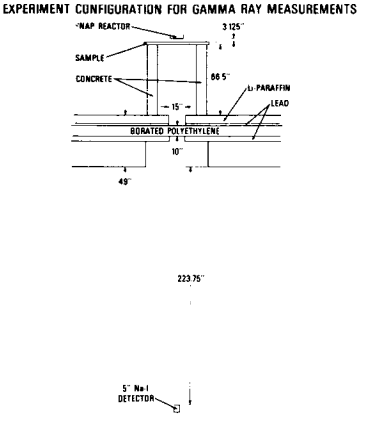

FIGURE 11.-Experimental Configuration for Gamma-Ray Measurements.

Calculations have been performed with DOT using a 27-neutron group - 60-gamma-ray group coupled library. Some of the calculations use the angular flux distribution beneath the reactor as a fixed boundary source for the slab shield calculations. In other cases, it has been necessary to calculate the reactor and shield as a single unit and include the effect of the shield on the power distribution in the reactor. The angular flux from the lower surface of the shield is integrated with the SPACE-TRAN code to determine the flux at the detector incorporating the uncollided flux attenuation of the borated polyethylene. The gamma-ray flux incident on the detector is folded with the detector response function so that the calculated pulse-height distribution is compared directly with the measurement.

Figure 12 shows the comparison of calculated and measured absolute pulse-height distribution for the bare core. The agreement below 4-1/2 MeV is excellent. Above 4-1/2 MeV, the experiment is high by almost a factor of 2. This disagreement is at present believed to be due to epithermal capture in structural materials in the reactor which are not adequately described. A comparison of dose or total energy flux would agree very well since the intensity is much greater at the lower energies.

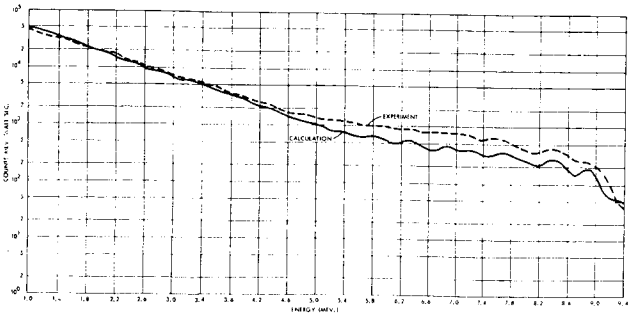

FIGURE 12.-Comparison of Calculated and Measured Gamma-Ray Pulse-Height Spectra From the Bare SNAP Reactor.

Figure 13 shows a comparison for experiment and calculation of the absolute pulse-height spectra for a 2-in. slab of heavimet placed directly under the SNAP reactor. Over most of the energy range the calculation is 20-25% low. At the higher energies above 7 MeV, the calculation is a factor of 2 low. However, the integral energy flux of the calculation and experiment agrees to within 15% due to the fact that the calculation agrees best with the experiment below 2 MeV where the intensity is the highest. This is the best comparison for any of the metal slabs.

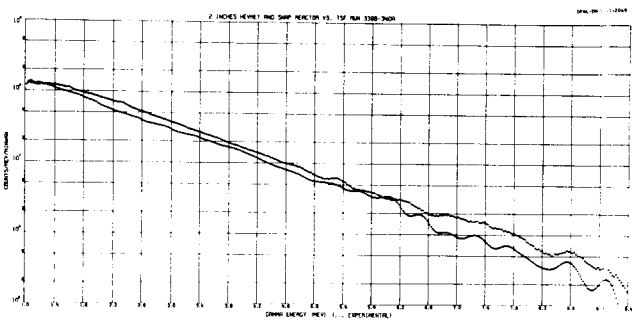

FIGURE 13.-Comparison of Calculated and Measured Gamma-Ray Pulse-Height Spectra From a 2-in. Heavimet Slab Under the SNAP Reactor.

The secondary gamma-ray production matrix used in this calculation, which included energy-dependent yields or epithermal capture, has been checked with the TSR-2 secondary gamma-ray experiment and shown to give substantially good results (ref. 19).

For the other gamma-ray shields the situation is not nearly so good. For lead, the TSR-2 gamma-ray experiments have shown that the secondary gamma-ray production data for neutron inelastic scattering is entirely inadequate. For uranium, the comparisons of calculation and measurements for the SNAP reactor experiments show that the calculations are low by about a factor of 2. This disagreement may be related to the anomaly in the neutron spectral comparisons since the TSR-2 gamma-ray experiment shows good agreement for ^{238}U foils.

In conclusion, the comparisons and calculations with the TSF-SNAP experiments have shown that the transport codes can accurately predict the neutron and gamma-ray radiation from the bare reactor. Also, the prediction of neutron transmission through shield slabs of lithium hydride, lead,and tungsten are adequately calculated. For secondary gamma-ray comparisons, the present status is not satisfactory in that relatively good agreement is only obtained for the heavimet alloy and tungsten powder assemblies.

The work presently in progress may soon resolve the difficulties experienced in neutron and gamma-ray comparisons for depleted uranium slabs, and the disagreement for lead constitutes a low priority problem in that lead has been ruled out as a likely candidate material in an actual SNAP shield.

Future experiments using the TSF-SNAP reactor will be for the verification of shield optimization by comparing measured and calculated dose derivatives and for verification of shield shaping procedures.

REFERENCES

1. MYNATT, F. R.; MUCKENTHALER, F. J.; and STEVENS, P. N.: Development of Two-Dimensional Discrete Ordinates Transport Theory for Radiation Shielding. USAEC Report CTC-INF-952, Union Carbide Corporation, 1969.
2. MYNATT, F. R.: A User's Manual for DOT. USAEC Report CCC-89, Union Carbide Corporation, 1969.
3. ENGLE, W. W., JR.: A Users Manual for ASOP, ANISN Shield Optimization Program. USAEC Report CTC-INF-941, Union Carbide Corporation, 1969.
4. STRAKER, E. A.; STEVENS, P. N.; IRVING, D. C.; and CAIN, V. R.: The MORSE Code - A Multigroup Neutron and Gamma-Ray Monte Carlo Transport Code. USAEC Report ORNL-4585, Oak Ridge National Laboratory, 1970.
5. MAERKER, R. E.; and MUCKENTHALER, F. J.: Gamma-Ray Spectra Arising From Thermal-Neutron Capture in Elements Found in Soils, Concretes, and Structural Materials. USAEC Report ORNL-4382, Oak Ridge National Laboratory, 1969.
6. FORD, W. E., III: The Use and "Testing" of Al, Fe, Ni, Cu, and Pb Secondary Gamma-Ray Production Data Sets from the POPOP4 Library. USAEC Report CTC-20, Union Carbide Corporation, 1970.
7. PENNY, S. K.; YOST, K. J.; and WHITE, J.: Calculation of Neutron-Capture Gamma-Ray Yields for Tungsten and Neutron Inelastic-Scattering Cross Sections for Iron. Transactions of the American Nuclear Society, Seattle, Washington, vol. 12, no. 1, pps. 386-388, 1969.
8. YOST, K. J.; WHITE, J. E.; and FU, C. Y.: Neutron Energy-Dependent Capture Gamma-Ray Yields for ^{238}U and ^{181}Ta. Transactions of the American Nuclear Society, Washington, D. C., vol. 13, no. 2, pps. 866-868, 1970.
9. ORPHAN, V.; and JOHN, J.: Intensities of Gamma Rays From the Radiative Capture in Natural Tungsten of Neutrons From 0.02 eV to 100 keV. Gulf General Atomic Report GA-9121, 1968.
10. JOHN, JOSEPH; and ORPHAN, V. J.: Gamma Rays From Resonant Capture of Neutrons in ^{238}U. Gulf General Atomic Report GA-10186, 1970.
11. ENGLE, W. W., Jr.: Optimization of a Shield for a Heat-Pipe-Cooled Fast Reactor Designed as a Nuclear Electric Space Power Plant. USAEC Technical Memorandum (to be published).
12. FORD, W. E., III: The POPOP4 Library and Codes for Preparing Secondary Gamma-Ray Production Cross Sections. This paper presented in this NASA document.
13. STRAKER, E. A.; CHILDS, R. L.; and EMMETT, M. B.: Application of DOT-MORSE Coupling to the Analysis of Three-Dimensional SNAP Shielding Problems. This paper presented in this NASA document.
14. BURGART, C. E.: MORSE Monte Carlo Shielding Calculations For the Zirconium Hydride Reference Reactor. This paper presented in this NASA document.
15. ENGLE, W. W., JR.: The Design of Asymmetric 4π Shields for Space Reactors. This paper presented in this NASA Document.
16. STRAKER, E. A.: Measurements of the Absolute Power and Fission Distribution in the TSF-SNAP Reactor and Comparison With Monte Carlo and Discrete Ordinates Calculations. USAEC Report ORNL-TM-2265, Oak Ridge National Laboratory, 1968.
17. CAIN, V. R.: Comparisons of Monte Carlo Calculations to Measurements of Neutron Leakage From the TSF-SNAP Reactor. USAEC Report ORNL-TM-2586, Oak Ridge National Laboratory, 1969.
18. GREENE, N. M.: Multigroup ^{6}Li and ^{7}Li Cross Sections. Paper 3.17 in Neutron Physics Division Annual Progress Report for Period Ending May 31, 1967. USAEC Report ORNL-4134, Oak Ridge National Laboratory, 1967.
19. FORD, WALTER E., III; and WALLACE, D. H.: Discrete-Ordinates Calculation of Secondary Gamma-Ray Spectra For Comparison with Tower Shielding Facility Experiments. Paper 2.22 in Neutron Physics Division Annual Progress Report For Period Ending May 31, 1969. USAEC Report ORNL-4433, Oak Ridge National Laboratory, 1969.